# THERMAL PROPERTIES OF POLYMER COMPOSITES FILLED WITH VARIOUS BIOPOLYMERS

Iveta Papučová, Petra Skalková*, Ivan Labaj, Jana Pagáčová, Mariana Pajtášová, Darina Ondrušová

Faculty of Industrial Technologies in Púchov, Alexander Dubček University of Trenčín, I. Krasku 491/30, 020 01 Púchov, Slovak Republic

**Abstract**

*For polymeric materials, the resistance to elevated or reduced temperatures is important. The thermal stability of a polymer determines its functional usability, and it is defined as a range of temperature, in which the polymer retains its elastic properties. The thermogravimetry was used for determination of thermal stability of biopolymers filled polymer composites. For observation of structural changes after the addition bio-fillers to polymer composites, the infrared spectroscopy was used. The most common biopolymers with interesting properties, which have been used as filler, are the cellulose, chitosan, galactomannan, starch and soy protein isolate. Natural rubber (NR) was blended with galactomannan (LBG), cellulose (CEL), chitosan (CHS) or soy protein isolate (SPI) as a filler in amount 0, 30 and 55 phr. The results indicate that the thermal degradation of NR/CEL, NR/CHS, NR/SPI and NR/LBG polymer composite in nitrogen is a three–step process. The first step is assigned the destruction of biopolymers. The second step is assigned to the decomposition of double bonds of methylene groups in polyisoprene molecules, i.e., to the decomposition of natural rubber. The third step is the carbonization of natural rubber.*

**Keywords:** *galactomannan, cellulose, chitosan, soy protein isolate, natural rubber, thermal stability, FTIR*

## 1. INTRODUCTION

Biopolymers are renewable source of raw materials of plant and animal origin. Recently, they have been used as potentially suitable fillers in polymer composites in order to substitute the inorganic fillers, mainly due to their biodegradation, their positive impact on the environment and the improvement of polymer composites properties. The cellulose [1-3], chitosan [4], galactomannan (Locust bean gum), starch [5] and soy protein isolate or glucose [6, 7] are the most common biopolymers with interesting properties to be used as filler.

The locust bean gum (LBG) is a galactomannan. The main chain consists of *β*–(1–4) linked mannose residues, and the side chains are *α*–(1–6) linked galactose. The ratio of the mannose to galactose in the chain is approximately 1:4 [8]. The soy protein is a globulin protein which is comprised in soybean oilseeds. The polypeptide chains of soy protein polymers are linked and entangled into a three-dimensional complicated structure by disulfide and hydrogen bonds. The production process includes the aqueous sublimation of protein and carbohydrates at neutral or alkaline pH. Subsequently, the sublimed protein is recovered, separated or even washed (rinsed) and neutralized before drying. The soy protein isolate is a cream coloured powder with 90–95% protein content [9]. Cellulose is the most abundant biomass on the earth and it is commonly used for the preparation of biobased nanomaterials [10]. Cellulose is a complex carbohydrate or polysaccharide, consisting of 3000 or more glucose units. As the basic structural component of plant cell walls, the cellulose comprises about 33% of all vegetable matter (90% of cotton and 50 % of wood are cellulose). Chitin is the second most ubiquitous natural polysaccharide on the earth. It is a white, hard, inelastic polysaccharide, found in exoskeletons but it is also in the internal structure of invertebrates. This biopolymer is a high molecular weight polysaccharide with a linear structure. Its structure contains an acetamide group ($–NHCOCH_3$). N–deacetylation of chitin, with, for example, sodium hydroxide, gives a chitin derivative – chitosan.

The use of biopolymers (natural and biodegradable fillers) in polymer composites is a suitable option for replacing rubber filler (carbon black). However, an important parameter is the amount of added biopolymer, because the biopolymer amount affects the properties of final polymer composite. The requirements for the properties of polymer composites have been increasingly higher and more demanding. The attention is mainly paid to the excellent mechanical, physico-chemical as well as thermal properties, including thermal stability predominantly [11]. In papers [1, 2, 7, 12, 13], the effect of biopolymers addition into the polymer composites on their mechanical, physical, chemical and thermal properties was studied. Addition of cellulose in polymer composites leads to the increase of tensile modulus of polymer composites [12]. The addition of bio-filler such as cellulose, soy protein isolate or chitosan increases mechanical properties of composites [2, 7, 13]. Polymer nanocomposites with cellulose have the higher thermal stability in comparison with neat rubber [1].

The work deals with the study of thermal and structural properties of natural rubber, pure biopolymers – galactomannan (Locust bean gum), soy protein isolate, cellulose and chitosan. The aim of this study was to determine how the amount as well as type of biopolymers affect the thermal and structural properties of polymer composites which are filled with mentioned biopolymers.

## 2. MATERIALS AND METHODS

### *2.1. Materials*

The materials were used as received: Natural rubber (NR) of SMR 10 was purchased from Kuala Lumphur, Malaysia. Galactomannan Locust bean gum (LBG), with DS 0.28, MW 310 000 g/mol, was purchased from Fluka Biochemica, England. Soy protein isolate (SPI) (90% protein content on dry basis, density min. 0.33 g/cm$^3$) was purchased from Green Medical, Czech Republic. Greencel GW70, cellulose fibres – Cellulose, (CEL) 99.5%, with bulk density 90-110 g/cm$^3$, was supplied from Bukóza Invest, Ltd. Slovak Republic. Chitosan (CHS), with degree of deacetylation 90%, density 600 kg/m$^3$, was purchased from Sigma-Aldrich Chemie, GmbH Germany.

### *2.2. Preparation of NR/biopolymer composites*

Four types of biopolymers, such as galactomannan (Locust bean gum), soy protein isolate, cellulose and chitosan, were melt-blended with natural rubber (NR) in Brabender Plasti – Corder PLE 331. Mixing process was performed at 80 and 90 °C and 50 rpm. The contents of biopolymer were 0, 30 and to 55 parts per hundred rubber (phr), respectively. Composites were vulcanized on the basis of the following formula: stearic acid, ZnO, Flavex, N–tert–butyl–2–benzothiazole sulfonamide and sulphur. The temperature of vulcanization was 150 °C.

### *2.3. Methods*

Thermogravimetric analysis was performed in the temperature range from 30 to 600 °C, using the Thermogravimetric Analyzer TGA/DSC 2 STARe system (Mettler Toledo, USA). The investigation process was performed under the following conditions: the heating rate 10 °C/min, nitrogen atmosphere while the sample mass from 20 to 30 mg was in $Al_2O_3$ crucible.

Infrared spectroscopy (FTIR) was performed with Nicolet iS50 FT-IR spectrometer (ThermoFisher Scientific, USA) with a resolution of 4 cm$^{-1}$ in the range of 400–4000 cm$^{-1}$ and ATR technique with diamond crystal.

## 3. RESULTS AND DISCUSSION

### *3.1. Thermal properties of biopolymers*

The thermal properties of biopolymers (Locust bean gum, soy protein isolate, cellulose, chitosan) as well as the thermal properties of natural rubber were studied, using thermogravimetric analysis. The thermogravimetric (TG/DTG) curves of investigated biopolymers and natural rubber are shown in the Figure 1.

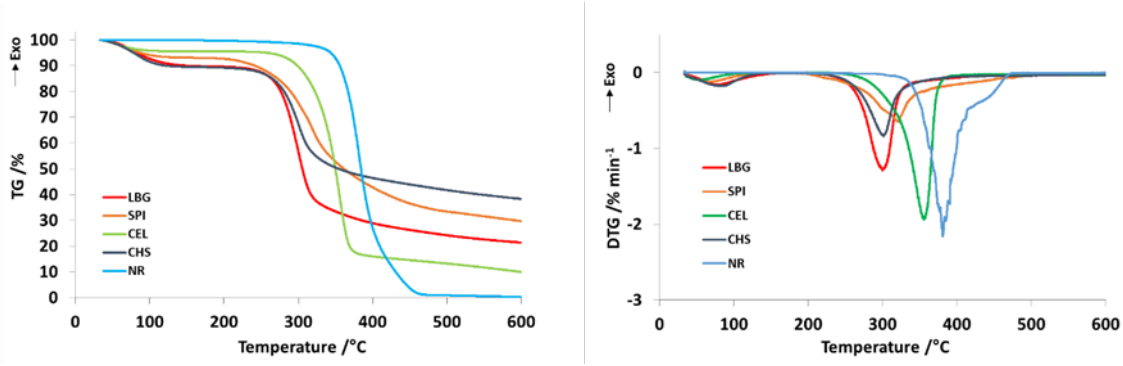



**Fig. 1.** TG (left) and DTG (right) curves of LBG, SPI, CEL, CHS and NR

The TG curve of pure galactomannan (LBG) (Fig. 1, red) shows mass loss in two stages. The first stage occurs at temperatures of 45–135 °C, 10.1% mass loss and it corresponds to the evaporation of adsorbed waters. The second stage of mass loss can be observed at temperatures of 244–314 °C and represents the decomposition of galactomannan (LBG). During the thermal decomposition of the biopolymer, 68.7% mass loss occurs. The DTG curve of pure LBG polysaccharide has two characteristic endothermic peaks at 79.8 °C and 300 °C.

In relation to the TG curve of pure soy protein isolate (Fig. 1, orange), two stages of mass loss can be seen. The first stage represents the loss of physically bound water at 50–105 °C and shows about 7.5 % mass loss. The second significant stage stands for the decomposition of soy protein isolate powder at temperatures of 223–335 °C and there is 64% mass loss observed. The DTG curve of soy protein isolate powder has two characteristic endothermic peaks at 78 and 316 °C [14].

The TG curve of the cellulose (Fig. 1, green) also shows mass loss in two stages. Slight mass loss (4.4%) in the region up to 112 °C is connected with the first stage of mass loss and it also corresponds the evaporation of water and volatile substances which are bound in the cellulose. The second stage of mass loss is observed at temperatures of 308–362 °C and it stands for the decomposition of cellulose and there is 86.5% mass loss. The DTG curve of the biopolymer cellulose has two characteristic endothermic peaks at 58 °C and 356 °C [15].

The TG curve of pure chitosan (Fig. 1, violet) exhibits two stages of mass loss. The first stage in the temperature range of 50–128 °C shows about 10.4% mass loss and it can be associated with the loss of adsorbed and bound water. The second stage can be seen at temperatures of 242–318 °C and it represents the degradation of chitosan as well as 51.6% mass loss. The DTG curve of the pure biopolymer has two characteristic endothermic peaks at 86 °C and 301 °C [4].

Based on the TG curve of pure natural rubber, there is two-stage degradation in nitrogen atmosphere. The first stage of decomposition at 340–410 °C represents the depolymerization of rubber and the second stage of decomposition in the temperature range of 410–450 °C represents the carbonization of NR. The total mass loss is 97.5% [7]. From the given DTG curve of the rubber (Fig. 1, blue), it is possible to see that the degradation of the natural rubber takes occurs at temperature of 380 °C.

All investigated biopolymers exhibit worse thermal stability in comparison with the natural rubber. The DTG curve of biopolymers and natural rubber (Fig. 1) shows that the thermal stability of investigated polymers is decreased in the following order: natural rubber, cellulose, soy protein isolate, chitosan and locust bean gum.

*3.2. Structural properties of biopolymers*

The structural properties of locust bean gum, soy protein isolate, cellulose, chitosan and natural rubber by Attenuated total reflectance-Fourier transform infrared (ATR-FTIR) spectroscopy were studied. FTIR spectra of investigated biopolymers are in Figure 2.

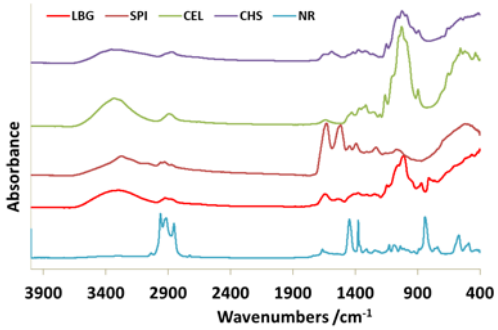



**Fig. 2.** FTIR spectra of LBG, SPI, CEL, CHS and NR

In spectra of locust bean gum (Fig. 2, red spectrum), the broad band between 3500 $cm^{-1}$ and 3100 $cm^{-1}$ was attributed to –OH stretching vibration formed by the hydroxyl group of polysaccharides and water. The band around 2800–3000 $cm^{-1}$ was attributed to C–H stretching vibration. FTIR spectrum exhibits the presence of characteristic bonds in the range of 2800–3000 $cm^{-1}$, 1540–1650 $cm^{-1}$ and 1050–1120 $cm^{-1}$ which correspond to the aliphatic, carboxylate and carbohydrate functions, respectively. The spectral range of 750–1300 $cm^{-1}$ corresponds to the carbohydrate's region. The band at ca. 871 $cm^{-1}$ is attributed to $\alpha$ and $\beta$ forms of galactose and mannose [16]. The peaks between 1037 and 1155 $cm^{-1}$ correspond to the stretching vibration of C–O and C–O–H bonds present in the glycosidic linkage of galactomannan [17].

For soy protein isolate (Fig. 7, brown spectrum), the absorption bands related to C=O stretching at 1629 $cm^{-1}$ (amide I), N–H bending at ca. 1515 $cm^{-1}$ (amide II) and C–H deformation at ca. 1447 $cm^{-1}$ were observed [18]. The absorption band at ca. 1234 $cm^{-1}$ is attributed to the C–N stretching and N–H bending (amide III) vibrations [19]. The band at ca. 1071 $cm^{-1}$ is due to the C–O stretching vibration. The bands at 2928 and 2958 $cm^{-1}$ correspond to $CH_2$ asymmetric stretching and $CH_3$ asymmetric stretching vibration, respectively. The C–H stretching vibration as well as stretching vibration of O–H and N–H groups are observed at 3065 and 3272 $cm^{-1}$, respectively [20].

In the absorbance spectra of cellulose (Fig. 7, green spectrum), there are the wide bands in the range from 3500 $cm^{-1}$ to 3200 $cm^{-1}$. They can be attributed to the stretching vibrations of the hydroxyl group of cellulose [2]. The band at 2892 and 2870 $cm^{-1}$ can be attributed to the methylene C–H asymmetric and symmetric stretching vibration, respectively [10]. The bands at 1332 and 1315 $cm^{-1}$ can be assigned to the bending of hydroxyl group (–OH) in cellulose [21]. The band at 1238 $cm^{-1}$ is associated with the C–H, O–H or $CH_2$ bending frequencies. The bands at 1049 and 896 $cm^{-1}$ correspond to the C–O stretching and C–H rocking vibrations of cellulose, respectively [2, 22].

For chitosan (Fig. 7, violet spectrum), absorption bands at 1058 and 1024 $cm^{-1}$ were observed, and they are associated C–N amino bonds. The absorption bands at 1641, 1589, and 1320 $cm^{-1}$ correspond to the amide–I, $–NH_2$ bending and amide–III, respectively. The absorption bands at 1149 $cm^{-1}$ (anti-symmetric stretching of the C–O–C bridge), 1058 and 1024 $cm^{-1}$ (skeletal vibrations involving the C–O stretching) are characteristic for the saccharide structure [23, 24]. The bands in the range from 3200 $cm^{-1}$ to 3500 $cm^{-1}$ can be attributed to the stretching vibration of O–H bonds.

In the absorption spectra of natural rubber (Fig. 7, blue spectrum), there is the broad band at 2960 $cm^{-1}$ and it can be attributed to the stretching vibrations of $CH_3$. The bands at 2920 and 2850 $cm^{-1}$ are assigned to the asymmetric and symmetric stretching vibrations of $CH_2$, respectively [25]. The absorption band at 1660 $cm^{-1}$ is attributed to the stretching C=C vibration. The bands at 1375 and 1360 $cm^{-1}$ correspond to the $CH_3$ asymmetric deformation. According to [26], the band at 1360 $cm^{-1}$ is related to the group cis–$C(CH_3)$=CH–. The band at 1120 $cm^{-1}$ belongs to C–C stretching vibrations and the band at ca. 1040 $cm^{-1}$ is assigned to $CH_3$ rocking vibrations, while the band at 745 $cm^{-1}$ belongs to $CH_2$ rocking vibrations. The peak at 1080 $cm^{-1}$ corresponds to $CH_2$ twisting deformation, the peak at 888 $cm^{-1}$ can

be attributed to =CH out of plane bending and the peak at 570 $cm^{-1}$ is related to C–C–C deformation [27].

*3.3. Thermal properties of biopolymers filled polymer composites*

Natural rubber was used as matrix for all prepared polymer composites. The all of the given biopolymers were used in amounts of 0, 30 and 55 phr as fillers in polymer composites and their thermal properties were observed in dependence on the amount of filler addition.

The Figs. 3–6 show the TG and DTG curves of polymer composites with 0, 30 and 55 phr of the filler - LBG, SPI, CEL and CHS, respectively. On the DTG curve (blue curve) of the polymer composites with 0 phr of filler we observe two degrees of decomposition. The first stage is in the temperature range of 290–410 °C and it corresponds to the decomposition of double bonds of methylene groups in polyisoprene molecules, i.e. to the decomposition of natural rubber. The second stage in temperature range of 410–455 °C can be assigned to the carbonization of rubber.

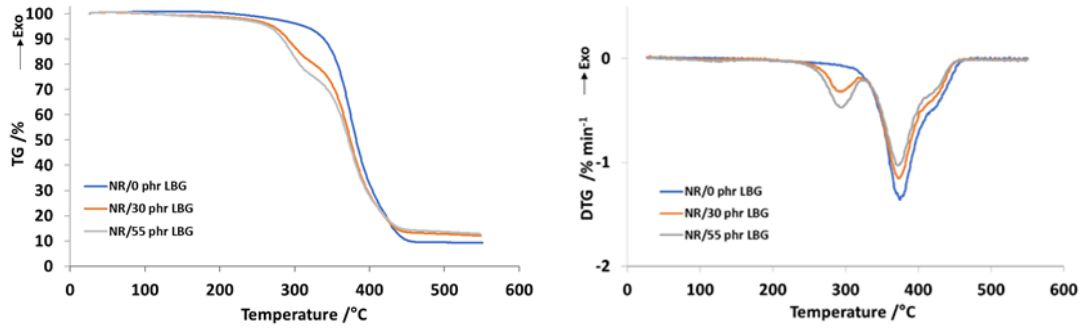



**Fig. 3.** TG (left) and DTG (right) curves of NR/LBG polymer composites with 0, 30 and 55 phr LBG

The curves of polymer composites with 30 and 55 phr of LBG (Fig. 3) exhibit three stages of decomposition. The first stage occurs at temperatures around 245–340 °C and this temperature range belongs to the decomposition of the LBG biopolymer. The second stage of decomposition occurs in the range of 340–410 °C and corresponds to the decomposition of natural rubber. The third stage occurs in the temperature range of 410–455 °C and it can be associated with the carbonization of the natural rubber. The temperature corresponding to the maximum of DTG curves is 377.9 and 375.9 °C for composite with 30 and 55 phr LBG, respectively. The increase of LBG filler amount in composites leads to the decrease of the total mass loss – it is 92 % for the composite with 0 phr of LBG, 88% for the composite with 30 phr of LBG and 86.3% for the composite with 55 phr. The thermal stability of polymer composites with LBG (galactomannan) is decreased due to the increase of LBG content.

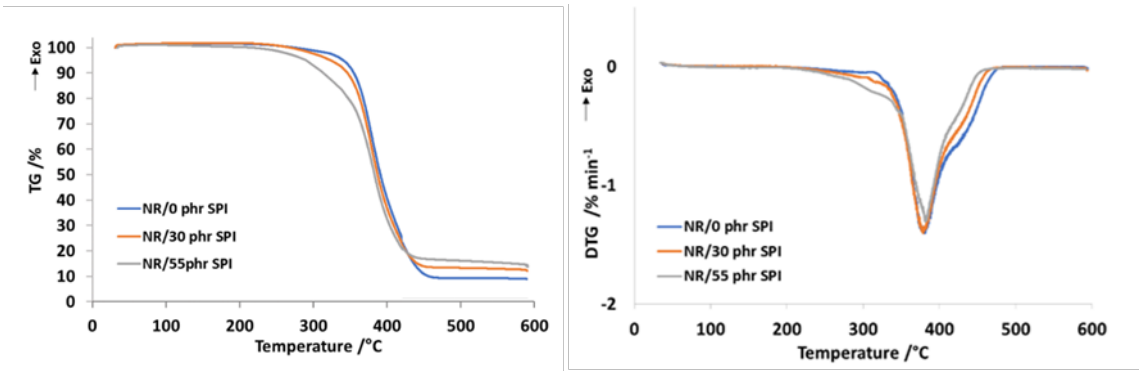



**Fig. 4.** TG (left) and DTG (right) curves of NR/SPI polymer composites with 0, 30 and 55 phr SPI

In the Fig. 4, three stages of decomposition can be seen from DTG curves of the NR/SPI polymer composites with 30 and 55 phr SPI. The first stage of decomposition of the polymer composites corresponds to the value of 260 °C and it can be assigned to the beginning of the decomposition of the soy protein isolate filler. The filler was decomposed up to 356 °C. The subsequent stage, at 360 °C, represents the beginning of the decomposition of natural rubber. At temperature of 378 °C and 381 °C for composites with 30 and 55 phr SPI, respectively, the double bonds of the methylene groups in the polyisoprene molecule are decomposed. The last stage can be seen in the temperature range of 410–460 °C, where the natural rubber is completely carbonized. With increasing amount of soy protein isolate in the composites, the total mass loss is decreased – it is 92% for the polymer composite with 0 phr of SPI, 88.2% for the composite with 30 phr of SPI and 85.6% for the composite with 55 phr of SPI. From the DTG curves, it is possible to see that the thermal stability of the polymer composites is increased along with increased filler content.

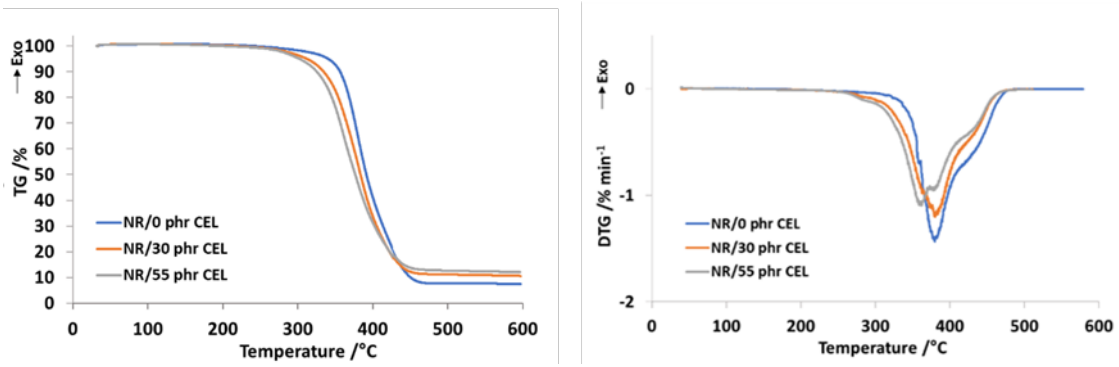



**Fig. 5.** TG (left) and DTG (right) curves of NR/CEL polymer composites with 0, 30 and 55 phr CEL

Three stages of decomposition are also observed in DTG curves of polymer composites filled with 30 and 55 phr CEL (Fig. 5). The first stage occurs at temperature range of 270–385 °C, this temperature range belongs to the decomposition of cellulose. The second stage of decomposition occurs in the range of 340–410 °C and corresponds to the decomposition of natural rubber. The third stage occurs in the temperature range of 410–465 °C and corresponds to the carbonization of the rubber. The temperature corresponding to the maximum of DTG curves is 379.6 °C and 377.6 °C for composite with 30 and 55 phr CEL, respectively. With increasing amount of cellulose filler in the composites, the total mass loss is decreased – it is 92% for the composite with 0 phr of CEL, 89.1% for the composite with 30 phr of CEL and 87.7% for the composite with 55 phr of CEL. From the DTG curves of the polymer composites filled with cellulose, it is possible to observe that the thermal stability of the polymer composites is decreases with increased filler content.

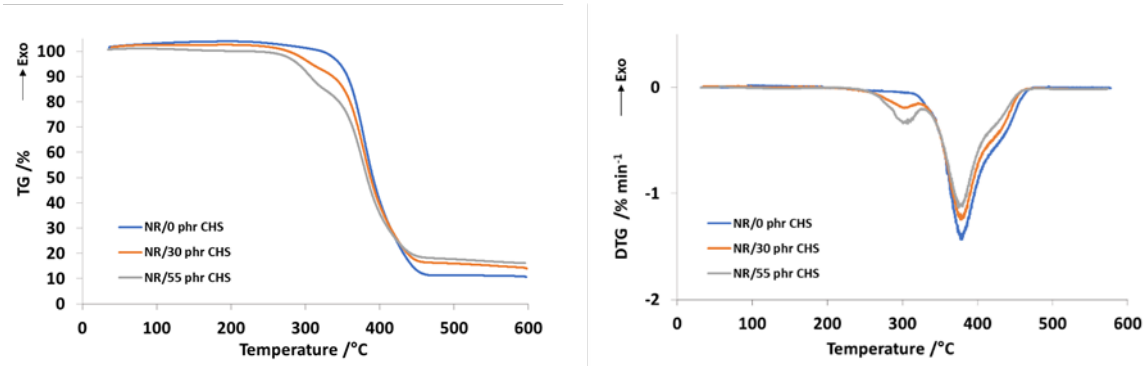



**Fig. 6.** TG (left) and DTG (right) curves of NR/CHS polymer composites with 0, 30 and 55 phr CHS

There are also three steps of decomposition in DTG curves of polymer composites with 30 and 55 phr CHS (Fig. 6). The first stage of the composite's decomposition can be observed at 260 °C and it corresponds to the beginning of the decomposition of the chitosan filler. The decomposition of the filler occurred to the temperature around 335 °C. The second stage of decomposition occurs in the range of 335–410 °C and it can be assigned to the decomposition of double bonds of methylene groups in polyisoprene molecules, i.e. to the decomposition of natural rubber. The third stage of decomposition can be observed in the temperature range of 410–465 °C and corresponds to the carbonization of the rubber. The temperature corresponding to the maximum of DTG curves is 379.2 °C and 377.3 °C for composites with 30 and 55 phr CHS, respectively. The increasing amount of chitosan filler in the composites leads to the decrease of the total mass loss – it is 92 % for the composite with 0 phr of CHS, 86.6% for the composite with 30 phr of CHS and 83.6% for the composite with 55 phr of CHS. From the DTG curves, it can be seen that the thermal stability of the polymer composites is decreased with increased filler content.

The effect of the biopolymer type in the polymer composites on the thermal stability was monitored for the completely filled polymer composites (maximum loading), i.e. 55 phr content of biopolymer. From the DTG curves in Fig. 7, it is possible to see that the thermal stability of polymer composites is decreased in the following order: NR/SPI, NR/CEL, NR/CHS and NR/LBG. All investigated composites showed sufficient thermal stability.

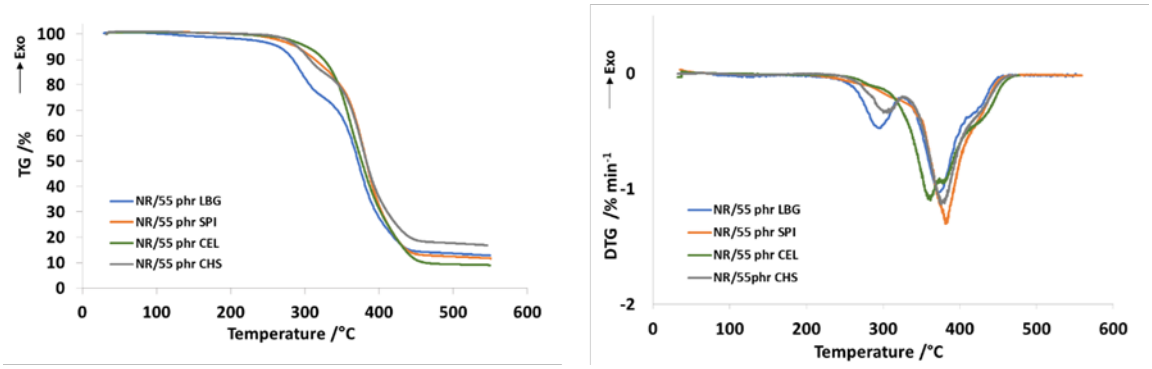



**Fig. 7.** TG (left) and DTG (right) curves of polymer composites with 55 phr LBG, 55 phr SPI, 55 phr CEL and 55 phr CHS

*3.4. Structural properties of biopolymers filled polymer composites*

For observation of structural changes after the addition biopolymers to polymer composite was used the infrared spectroscopy. The Fig. 8 shows the FTIR spectra of NR composite with different LBG filler contents. The increase of filler content leads to the slight increase in intensity of the free hydroxyl groups at 3280 $cm^{-1}$ and it is due to the presence of the LBG filler. The intensity of the bands at 2920 and 2850 $cm^{-1}$, which correspond to the vibrations of the methylene groups, was increased in the composites depending on the amount of LBG filler. The spectra show differences in band intensity at 1550 $cm^{-1}$ and 1540 $cm^{-1}$. This region includes galactose and mannose. In the spectral region around 1120 $cm^{-1}$, 1040 $cm^{-1}$ and 743 $cm^{-1}$, the decrease in the intensity of the bands for natural rubber can be seen and it can be attributed to the increasing content of locust bean gum in composites.

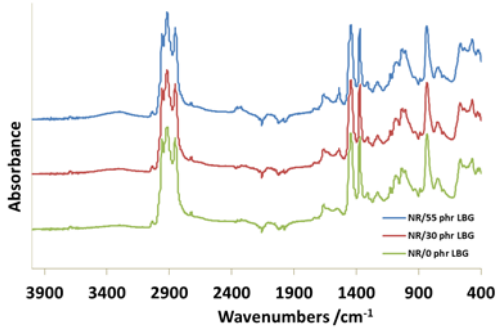



**Fig. 8.** FTIR spectra of NR/LBG polymer composites with 0, 30 and 55 phr LBG

The Fig. 9 shows the FTIR spectra of NR polymer composites with different contents of the soy protein isolate filler. The increase of the filler content leads to slight increase in intensity of band around 3280 $cm^{-1}$ (free hydroxyl groups) and it is due to the presence of the filler. The intensity of the bands belonging to the natural rubber decreases in the range of 2960–2850 $cm^{-1}$ with increasing amount of filler. The same can be seen for the bands at 1375 $cm^{-1}$, 1120 $cm^{-1}$ and 720 $cm^{-1}$. The spectra show the gradual increase in the intensity of the bands belonging to the soy protein isolate at 1630 $cm^{-1}$ and 1520 $cm^{-1}$ and it is due to increasing amount of filler.

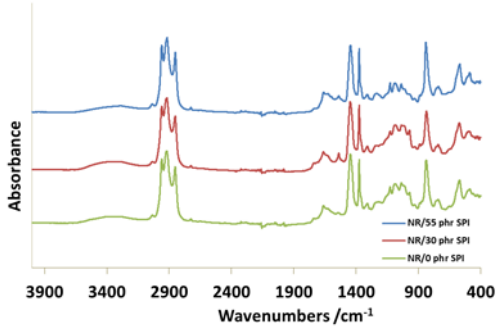



**Fig. 9.** FTIR spectra of NR/SPI polymer composites with 0, 30 and 55 phr SPI

In the Fig. 10, there are the FTIR spectra of NR/CEL polymer composites. In the region of 3200–3600 $cm^{-1}$, the bands belonging to the stretching vibration of O–H groups can be seen. The presence of these bands indicates the presence of the cellulose filler. The increase in filler content leads to the slight increase of the intensity of these bands. The intensity of the bands, which correspond to the stretching vibrations of the natural rubber, is changed with the cellulose content: the intensity of the bands at 2960 $cm^{-1}$, 2850 $cm^{-1}$, 2920 $cm^{-1}$, 745 $cm^{-1}$ and 570 $cm^{-1}$ is decreased when the amount of cellulose filler is increased. The intensity of the bands belonging to the cellulose at 890 $cm^{-1}$ and 1040 $cm^{-1}$ is increased with the increase of filler amount.

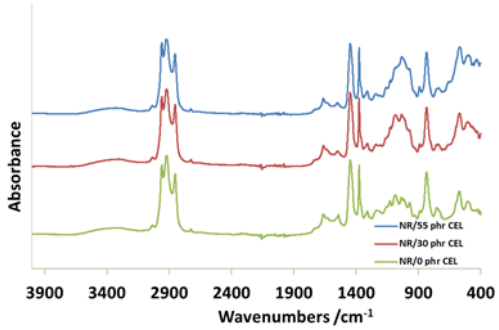



**Fig. 10.** FTIR spectra of NR/CEL polymer composites with 0, 30 and 55 phr CEL

In the Fig. 11, there are the FTIR spectra of polymer composites, which are filled with chitosan. The increase of the filler content leads to slight increase in the band intensity of the free hydroxyl groups in the range of 3200–3500 $cm^{-1}$ and it is due to the presence of the filler. The intensity of the bands in the spectral range from 1020 $cm^{-1}$ to 1090 $cm^{-1}$ is increased in direct proportion to the increasing content of CHS filler in the polymer composites and it can be attributed to the N–C bonds in the amino groups. The intensity of the bands at 2960 $cm^{-1}$ and 2850 $cm^{-1}$, belonging to the vibrations of the natural rubber, is decreased slightly with the content of chitosan filler.

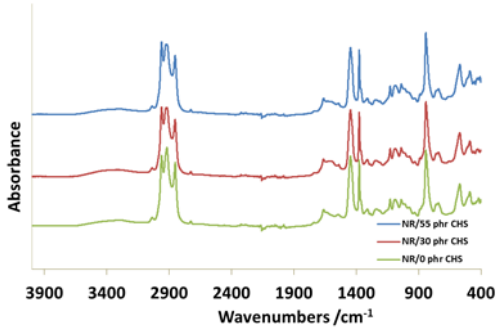



**Fig. 11.** FTIR spectra of NR/CHS polymer composites with 0, 30 and 55 phr CHS

## 4. CONCLUSIONS

The given work includes the preparation of polymer composites with different types of biopolymers as well as determination of the effect of the type and amount of biopolymer on thermal and structural properties. By observing the thermal behaviour of selected types of fillers, it was possible to determine and specify that the thermal stability of pure biopolymers is decreased in the following the order: cellulose, soy protein isolate, chitosan and locust bean gum. Based on the thermal behaviour of the prepared polymer composites, it is possible to conclude that all of composites exhibited sufficient thermal stability. In the case of NR polymer composites with cellulose, chitosan and locust bean gum, the thermal stability of the composites was decreased slightly with the increase of filler amount. In comparison with the given mentioned composites, the polymer composites with the soy protein isolate showed the improvement of thermal stability after the filler content had been increased. Relating to the mutual comparison of the thermal stability for individual composites with maximum loading (maximum amount of filler – 55 phr of the soy protein isolate, cellulose, chitosan and locust bean gum), it was found out that the composite of NR/SPI exhibited the best thermal stability and then there was the slight sequential decrease in the following order: NR/CEL, NR/CHS and NR/LBG, respectively. The characteristic bonds/vibrations of the given filler (LBG, SPI, CHS and CELL) as well as NR in the polymer composites were identified by FTIR spectroscopy.

**ACKNOWLEDGMENTS**

This research work has been supported by the Operational Programme Integrated Infrastructure, co-financed by the European Regional Development Fund by the project: Advancement and support of R&D for "Centre for diagnostics and quality testing of materials" in the domains of the RIS3 SK specialization, Acronym: CEDITEK II., ITMS2014+ code 313011W442.

**REFERENCES**

1. Oboh, JO, Okafor, JO, Kovo, AS, Abdulrahman, AS 2017, "Investigation of eco-friendly cellulosic nanoparticles potential as reinforcement agent in the production of natural rubber composites", *Nigerian Journal of Technology*, vol. 36, no. 4, pp. 1078-1087.
2. Abraham, E, Deepa, B, Pothan, LA, John, M, Narine, SS, Thomas, S, Anandjiwala R 2013, "Physicomechanical properties of nanocomposites based on cellulose nanofibre and natural rubber latex", *Cellulose*, vol. 20, no. 1, pp. 417-427.
3. Singh, S, Dhakar, GL, Kapgate, BP, Maji, PK, Verma, C, Chhajed, M, Rajkumar, K, Das, C 2020, "Synthesis and chemical modification of crystalline nanocellulose to reinforce natural rubber composites", *Polymer for Advanced Technologies*, vol. 31, no. 12, pp. 3059-3069.
4. Johns, J, Rao, V 2008, "Characterization of Natural Rubber Latex/Chitosan Blends", *International Journal of Polymer Analysis and Characterization*, vol. 13, no. 4, pp. 280-291.
5. Wang, ZF, Peng, Z, Li, SD, Lin, H, Zhang, KX, She, XD, Fu, X 2009, "The impact of esterification on the properties of starch/natural rubber composite", *Composites Science and Technology*, vol. 69, no. 11-12, pp. 1797-1803.
6. Nimpaiboon, A, Sakdapipanich, J 2013, "A model study on effect of glucose on the basic characteristics and physical properties of natural rubber", *Polymer Testing*, vol. 32, no. 8, pp. 1408-1416.
7. Jong, L 2015, "Influence of protein hydrolysis on the mechanical properties of natural rubber composites reinforced with soy protein particles", *Industrial Crops and Products*, vol. 65, pp. 102-109.
8. Prajapati, VD, Jani, GK, Moradiya, NG, Randeria, NP, Nagar, BJ, Naikwadi, NN, Variya, BC 2013, "Galactomannan: A versatile biodegradable seed polysaccharide", *International Journal of Biological Macromolecules*, vol. 65, pp. 83-92.
9. Kumar, R, Choudhary, V, Mishra, S, Varma, IK, Mattiason, B 2002, "Adhesives and plastics based on soy protein products", *Industrial Crops and Products*, vol. 16, no.3, pp. 155-172.
10. Agrebi, F, Ghorbel, N, Bresson, S, Abbas, O, Kallel, A 2018, "Study of nanocomposites based on cellulose nanoparticles and natural rubber latex by ATR/FTIR spectroscopy: The impact of reinforcement", *Polymer Composites*, vol. 4, no. 5, pp. 2076-2087.
11. Jovanović, S, Jovanović, V, Marković, G, Samaržija-Jovanović, S, Milićević, Z, Marinović-Cincović, M, Budinski-Simendić, J 2019, "Elastomers based on NR/BR/SBR ternary rubber blend: Morphological, mechanical and thermal properties". *Chemical Industry & Chemical Engineering Quarterly*, vol. 25, no. 1, pp. 31-38.
12. Santos, D, Iulianellig, FA, Tavares, CV 2016, "The use of cellulose nanofillers in obtaining polymer nanocomposites: properties, processing and applications", *Materials Sciences and Applications*, vol. 7, no. 5, pp. 257-294.
13. Rao, V, Johns, J 2007, "Mechanical properties of thermoplastic elastomeric blends of chitosan and natural rubber latex", *Journal of Applied Polymer Science*, vol.107, no. 4, pp. 2217-2223.

14. Ryan, M, McEvoy, E, Duignan, S, Crowley, C, Fenelon, M, O'Callaghan, D M, FitzGerald, R J 2008, "Thermal stability of soy protein isolate and hydrolysate ingredients", *Food Chemistry*, p. 108, no. 2, pp. 503-510.
15. Szcześniak, L, Rachocki, A, Tritt-Goc, J 2007, "Glass transition temperature and thermal decomposition of cellulose powder", *Cellulose*, vol. 15, no. 3, pp. 445-451.
16. Martins, JT, Cerqueira, MA, Bourbon, AI, Pinheiro, AC, Souza, BWS, Vicente, AA 2012, "Synergistic effects between κ-carrageenan and locust bean gum on physicochemical properties of edible films made thereof", *Food Hydrocolloids*, vol. 29, no. 2, pp. 280-289.
17. Cerqueira, MA, Souza, BWS, Simões, J, Teixeira, JA, Domingues, MRM, Coimbra, MA, Vicente, AA 2011, "Structural and thermal characterization of galactomannans from non-conventional sources", *Carbohydrate Polymers*, vol. 83, no. 1, pp. 179-185.
18. Kumar, R, Anandjiwala, RD, Kumar, A 2016, "Thermal and mechanical properties of mandelic acid-incorporated soy protein films", *Journal of Thermal Analysis and Calorimetry*, vol. 123, no. 2, pp. 1273-1279.
19. Kumar, R, Wang, L, Zhang, L 2008, "Structure and mechanical properties of soy protein materials plasticized by Thiodiglycol", *Journal of Applied Polymer Science*, vol. 111, no. 2, pp. 970-977.
20. Chen, X, Ru, Y, Chen, F, Wang, X, Zhao, X, Ao, Q 2013, "FTIR spectroscopic characterization of soy proteins obtained through AOT reverse micelles", *Food Hydrocolloids*, vol. 31, no. 2, pp. 435-437.
21. Colom, X, Carrasco, F, Pagè, P, Cañavate, J 2003, "Effects of different treatments on the interface of HDPE /lignocellulosic fiber composites", *Composites Science and Technology*, vol. 63, no. 2, pp. 161-169.
22. Alemdar, A, Sain, M 2008, "Isolation and characterization of nanofibers from agricultural residues - Wheat straw and soy hulls", *Bioresource Technology*, vol. 99, no. 6, pp. 1664-1671.
23. Rahim, M, Mas Haris MRH 2021, "Green biocomposites of chitosan dispersed in natural rubber matrices, and their urea controlled-release application", *Materials Today Chemistry*, vol. 19, pp. 100401.
24. Peniche, C, Argüelles-Monal, W, Davidenko, N, Sastre, R, Gallardo, A, San Román J 1999, "Self-curing membranes of chitosan/PAA IPNs obtained by radical polymerization: preparation, characterization and interpolymer complexation", *Biomaterials*, vol. 20, no. 20, pp. 1869-1878.
25. Dinsmore, HL, Smith, DC 1998, "Analysis of natural and synthetic rubber by infrared spectroscopy", *Analytical Chemistry*, vol. 20, no. 2, pp. 11-24.
26. Bart, A 2007, "Infrared spectroscopy of proteins", *Biochimica et Biophysica Acta*, vol. 1767, no. 44, pp. 1073-1101.
27. Yu, H, Zeng, Z, Lu, G, Wang, Q 2008, "Processing characteristics and thermal stabilities of gel and sol of epoxidized natural rubber", *European Polymer Journal*, vol. 44, no. 2, pp. 453-464.